

# A New ATP-Sensitive K<sup>+</sup> Channel–Independent Mechanism Is Involved in Glucose-Excited Neurons of Mouse Arcuate Nucleus

Xavier Fioramonti,<sup>1</sup> Anne Lorsignol,<sup>1</sup> Anne Taupignon,<sup>2</sup> and Luc Pénicaud<sup>1</sup>

Glucose is known to modify electrical activity of neurons in different hypothalamic areas such as the arcuate nucleus (ARC) or the ventromedian nucleus. In these structures, it has been demonstrated that glucose-induced excitation of neurons involves ATP-sensitive K<sup>+</sup> (K<sub>ATP</sub>) channel closure. The aim of the present study was to determine whether ARC neurons were able to detect high extracellular glucose concentrations and which mechanisms were involved in this detection by using whole-cell and cell-attached patch-clamp techniques in acute mouse brain slices. An increase from 5 to 20 mmol/l glucose stimulated 19% and inhibited 9% of ARC neurons. Because of the high-glucose concentrations used, we called these neurons high-glucose-excited (HGE) and high-glucose-inhibited (HGI) neurons, respectively. Glucose-induced depolarization of HGE neurons was not abolished by tetrodotoxin treatment and was correlated with an increase of membrane conductance that reversed at ~20 mV. Experiments with diazoxide, pinacidil, or tolbutamide showed that K<sub>ATP</sub> channels were present and functional in most of the ARC neurons but were mostly closed at 5 mmol/l glucose. Moreover, HGE neurons were also present in ARC of Kir6.2 null mice. These results suggested that ARC neurons have the ability to sense higher glucose concentrations than 5 mmol/l through a new K<sub>ATP</sub> channel-independent mechanism. *Diabetes* 53:2767–2775, 2004

The hypothalamus contributes to the control of energy homeostasis by integrating metabolic information and eliciting adaptive responses. The arcuate nucleus (ARC) plays a pivotal role in this control (1–3). Indeed, ARC neurons release neuromodulators of food intake (4) and are located just above the median eminence, a highly vascularized structure with many capillary loops and fenestrated endothelial cells (5). This location allows this nucleus to easily integrate periph-

eral signals of body energy status into changes in neuronal activity (6,7).

The role of glucose as a signal that informs the hypothalamus about body energy status has been investigated by different groups (8). Several studies demonstrated that an intracarotid injection of glucose at a concentration that did not modify peripheral glycemia induced *c-fos* activation in hypothalamic nuclei such as the ARC and triggered a rapid and transient insulin secretion, indicating that the brain senses and regulates glucose homeostasis (9,10). Moreover, it has been shown that an intravenous injection of glucose modified electrical activity of neurons located in the lateral hypothalamus or in the ventromedian hypothalamus (VMH), which contains both the ARC and the ventromedian nucleus (VMN) (11,12). Since that time, glucosensing neurons whose electrical activity may be modified by changes in extracellular glucose concentration have been identified by patch-clamp on hypothalamic slices (7,13–16). Glucose-excited or -inhibited neurons increase or decrease their electrical activity, respectively, as extracellular glucose concentration increases (16).

Whereas the mechanism whereby glucose-inhibited neurons sense glucose is unclear, glucose-excited neurons would use the ATP-sensitive K<sup>+</sup> (K<sub>ATP</sub>) channels to respond to glucose (17). This is similar to pancreatic  $\beta$ -cells, where hyperglycemia is detected via a system involving the glucose transporter GLUT2 coupled to glucokinase and K<sub>ATP</sub> channels (18). K<sub>ATP</sub> channels are widely distributed throughout the brain (19) and are present in VMN and ARC glucose-excited neurons (20–22). The glucose-induced activation of these glucose-excited neurons was mimicked by sulfonylureas (K<sub>ATP</sub> channel blockers) and correlated with a decrease of K<sup>+</sup> conductance (7,13–16). However, both in pancreatic  $\beta$ -cells and in hypothalamus, a K<sub>ATP</sub> channel-independent mechanism underlying glucose effect has been suggested (23–26).

Extracellular brain glucose concentration seems to be lower than that of plasma glucose (27). However, the location of the ARC near the median eminence makes it likely that glucose concentrations in this region may approach plasma levels. ARC glucosensing neurons have predominantly been characterized using large steps in glucose concentration from 0 to 10 or 20 mmol/l (13–15). However the brain would never be exposed to such a single-step increase in glucose concentration but rather would see more gradual changes above and below some steady-state level. Below 5 mmol/l, the sensitivity of ARC glucosensing neurons to glucose has been examined in

From <sup>1</sup>CNRS UMR 5018, Paul Sabatier University, Toulouse, France; and <sup>2</sup>CNRS UMR 5543, Victor Segalen University, Bordeaux, France.

Address correspondence and reprint requests to Dr. Anne Lorsignol, UMR 5018 CNRS-UPS, IFR 31, CHU Rangueil, 1 Avenue Jean Poulhès, 31403 Toulouse, France. E-mail: anne.lorsignol@toulouse.inserm.fr.

Received for publication 8 June 2004 and accepted in revised form 30 July 2004.

ARC, arcuate nucleus; HGE, high glucose excited; HGI, high glucose inhibited; K<sub>ATP</sub> channel, ATP-sensitive K<sup>+</sup> channel; TTX, tetrodotoxin; VMH, ventromedian hypothalamus; VMN, ventromedian nucleus.

© 2004 by the American Diabetes Association.

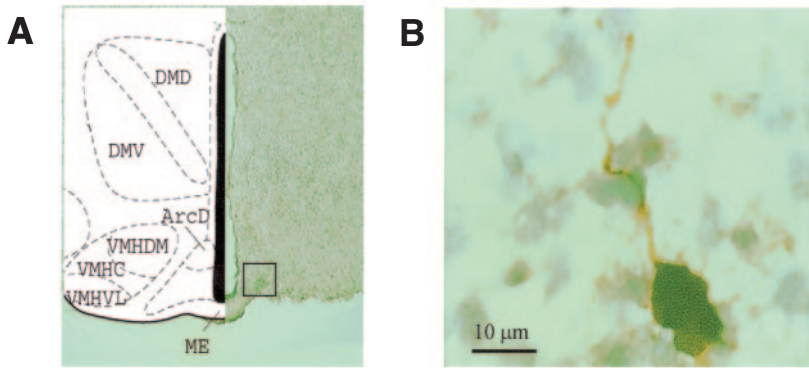


**FIG. 1.** ARC location of recorded neurons. **A:** Coronal view of location of recordings. **B:** Magnification of the square drawn in **A**, showing a neurobiotin-labeled neuron.

detail (7). Above 5 mmol/l, the presence of glucosensing neurons has been shown (22,28,29), but the underlying mechanism has been poorly investigated. Thus, the aims of the present study were to characterize in ARC neurons 1) their biophysical properties and 2) the intracellular mechanisms in response to an increase in extracellular glucose concentration from 5 to 20 mmol/l.

## RESEARCH DESIGN AND METHODS

**Brain slice preparation.** All experiments were carried out in nonfasted mice in accordance with European Community guidelines. Electrophysiological recordings were performed on hypothalamic slices from 19- to 22-day-old male C57BL/6J mice. After cervical dislocation, the brain was quickly removed and immersed in an ice-cold oxygenated (95% O<sub>2</sub>/5% CO<sub>2</sub>) saline solution that contained (in mmol/l) 200 sucrose, 28 NaHCO<sub>3</sub>, 2.5 KCl, 7 MgCl<sub>2</sub>, 1.25 NaH<sub>2</sub>PO<sub>4</sub>, 0.5 CaCl<sub>2</sub>, 1 L-ascorbate, and 8 D-glucose (pH 7.4). Three 300- $\mu$ m coronal slices per brain were cut in this solution. Slices were then incubated at room temperature in oxygenated extracellular medium that contained (in mmol/l) 118 NaCl, 3 KCl, 1 MgCl<sub>2</sub>, 25 NaHCO<sub>3</sub>, 1.2 NaH<sub>2</sub>PO<sub>4</sub>, 1.5 CaCl<sub>2</sub>, 5 HEPES, and 5 D-glucose, and 15 sucrose (osmolality adjusted at 300–310 mOsmol/l [pH 7.4]) for a 1-h recovery period.

Some experiments used homozygous K<sub>ATP</sub> channel-deficient mice (Kir6.2<sup>-/-</sup>) that were generated by disruption of the *Kir6.2* gene (30). Slices from 19- to 22-day-old male Kir6.2<sup>-/-</sup> mice were prepared.

**Patch-clamp recordings.** Slices were transferred into a recording chamber on the stage of an upright microscope (Nikon), immobilized by a nylon grid, and perfused at 2–3 ml/min with the extracellular medium. The ARC was identified by using the mouse brain stereotaxic atlas (31). ARC neurons were visualized using a  $\times 60$  water immersion objective (Nikon) under infrared differential interference contrast illumination and an infrared video camera (Hamamatsu Photonics).

Borosilicate pipettes (5–7 M $\Omega$ ; GC150F-10, Phymep) were filled with an internal solution that contained (in mmol/l) 130 K-gluconate, 0.1 EGTA, 1 CaCl<sub>2</sub>, 10 HEPES, 5 Mg-ATP, and 0.4 Na-GTP (pH and osmolality adjusted at 7.25 and 290 mOsmol/l, respectively) for whole-cell recordings or with filtered extracellular medium for cell-attached recordings. Recordings were made using an Axopatch 1D amplifier (Axon Instruments), digitized using the Digidata 1320A interface, and acquired using pClamp 8.2 software (Axon Instruments). The amplifier filter was set at 5 kHz for whole-cell current-clamp recordings and at 2 kHz for whole-cell voltage-clamp or cell-attached recordings. Pipettes and cell capacitances were fully compensated. Junction potential was calculated using pClamp 8.2 and corrected off-line.

**Drugs and glucose application.** Glucosensing neurons were identified using extracellular medium that contained 20 mmol/l D-glucose and 0 mmol/l sucrose (300–310 mOsmol/l [pH 7.4]).

D-Glucose, cesium chloride, tolbutamide, and diazoxide were purchased from Sigma; pinacidil was purchased from Tocris; and tetrodotoxin (TTX) was purchased from Latoxan. All (except for the D-glucose) were prepared as concentrated stock solution and stored at  $-80^{\circ}\text{C}$ . When drugs (diazoxide, pinacidil, and tolbutamide) were prepared in DMSO, the final concentration of solvent was always kept below 0.001. Drugs that were diluted in oxygenated extracellular medium were delivered at 2 ml/min by a multibarrel gravity-feed system (ALA Scientific Instruments, Segre Electronique) positioned at  $\sim 2$  mm from the ARC. Drug wash-in occurred within 2 and 10 s as measured by application of high potassium solution.

**Histochemistry protocol.** The location of recorded cells was determined via diffusion of neurobiotin (0.2% in the whole-cell pipette solution; Vector

Laboratories) into the cytosol. After recording, brain slices were fixed in 4% paraformaldehyde/0.2% picric acid in PBS for 90 min at room temperature. Slices were then cryoprotected in 20% sucrose for at least 12 h at 4 $^{\circ}\text{C}$  and frozen at  $-60^{\circ}\text{C}$  in isopentane (Prolabo). Slices (300  $\mu$ m) were then cut into 16- $\mu$ m serial sections using a cryostat (Leica) and collected on microscope slides (Menzel-Glaser). After quenching peroxidase activity with 0.1% H<sub>2</sub>O<sub>2</sub> for 20 min at room temperature, sections were incubated in PBS/0.3% triton X100 (Sigma)/3% normal goat serum (Sigma) for 30 min at room temperature. Neurobiotin was then detected by incubation in streptavidin-peroxidase conjugate (1:4,000; Jackson Laboratories) for 90 min at room temperature. Afterward, peroxidase activity was revealed by diaminobenzidine (DakoCytomation). After hematoxylin counterstaining (Shandon) and alcohol dehydration, sections were cleared in Bioclear (MicroStain [*n*-limonene]; Micron) and examined under a transmitted-light microscope (Leica).

**Data analysis and representation.** Recordings were analyzed using pClamp 8.2 and Clampfit 8.2 software (Axon Instruments) and plotted with Origin 5.0 (Microcal Software). Data were shown as mean  $\pm$  SE, and differences between groups were analyzed by paired or unpaired Student's *t* test, with  $P < 0.05$  taken as significant.

In illustrations of current-clamp experiments, resting membrane potential was systematically indicated by a dotted line and mentioned on the right of each trace. All action potentials were truncated at 10 mV. For long recordings (in the case of glucose responses), data were acquired and shown in episodic mode with 10-s sweeps.

## RESULTS

**Biophysical properties of arcuate neurons.** A total of 308 neurons in the median and anterior arcuate (ARC) were studied under current-clamp and voltage-clamp analysis in this study (Bregma coordinates between  $-1.46$  and  $-2.18$  mm in adult mice [31]). This location was confirmed by postrecording detection of neurobiotin-labeled neurons (Fig. 1).

ARC neurons had a mean membrane capacitance of  $28.3 \pm 1.3$  pF, and their input resistance ranged from 150 to 3,000 M $\Omega$ . In control conditions (i.e., 5 mmol/l glucose in extracellular medium), 88% of ARC neurons presented a spontaneous activity. Two subpopulations of active neurons could be distinguished: 17% presented a regular pattern of firing rate with a mean action potential frequency of  $8.0 \pm 0.70$  Hz; the 83% remaining active neurons showed an irregular bursting pattern. Current-clamp analysis revealed that  $>80\%$  of ARC-recorded neurons received excitatory and/or inhibitory presynaptic input.

Triggered hyperpolarizing current injections were performed to investigate membrane properties of ARC neurons. Five distinct electrical phenotypes thus could be distinguished. Types A, B, and C neurons similar to those described by Burdakov and Ashcroft (32) were identified. Twenty-five percent of ARC neurons (79 of 308) immediately resumed normal firing after hyperpolarizing current injection and corresponded to type A neurons (Fig. 2A);

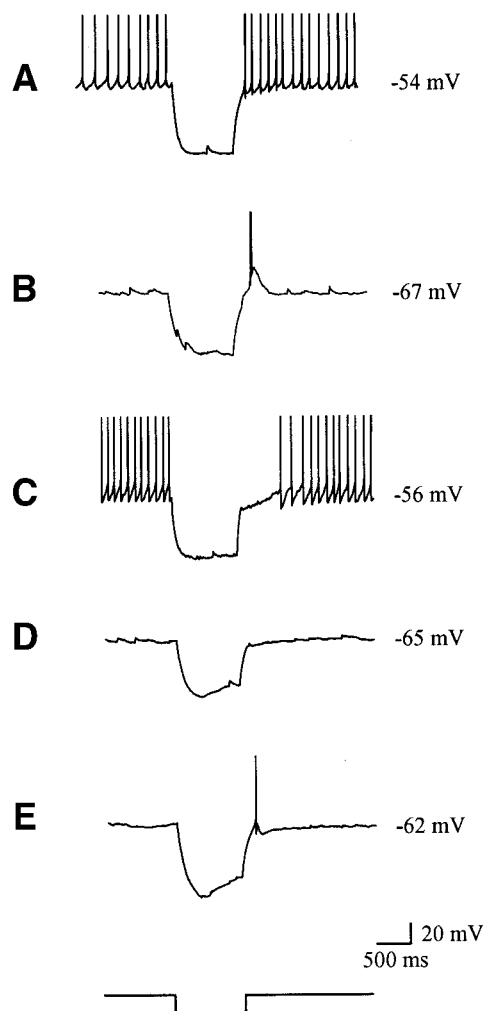


**FIG. 2.** Five electrical phenotypes are found in the ARC. Hyperpolarizing current injections ( $-10$  to  $-80$  pA) were used to distinguish neuron subpopulations. Current step is schematically displayed below the records. *A, B, C, D,* and *E* illustrate types *A, B, C, D,* and *E* neurons, respectively.

34% (106 of 308; type B neurons) showed a rebound depolarization at the end of hyperpolarizing current injections (Fig. 2*B*), and 5% (15 of 308; type C neurons) displayed a rebound hyperpolarization that caused them to resume firing with a delay of  $742 \pm 115$  ms (Fig. 2*C*). However, two other electrical phenotypes were also identified: 9% (27 of 308; type D neurons) showed a “sag” in membrane potential (Fig. 2*D*), and 26% (81 of 308; type E neurons) showed a “sag” and a rebound depolarization (Fig. 2*E*). Voltage-clamp steps from  $-70$  to  $-150$  mV on both of these neuron subtypes revealed a hyperpolarizing-activated inward ( $I_h$ ) current (Fig. 3*A, right*). Both “sag” in membrane potential and  $I_h$  current were reversibly blocked by external  $\text{Cs}^+$  ( $4$  mmol/l) application (Fig. 3*B*). This pharmacological approach confirmed the presence of  $I_h$  current in types D and E ARC neurons.

#### **Presence of glucosensing neurons in the mouse ARC.**

A transient glucose increase from  $5$  to  $20$  mmol/l was used to identify glucosensing neurons in the ARC. Whole-cell recordings revealed that this  $5$ - to  $20$ -mmol/l glucose step modified electrical activity in 26% (35 of 135) of ARC neurons. The 74% remaining cells were defined as glucose-

insensitive neurons. Glucose responses usually appeared with a delay (ranging from  $30$  s to  $3$  min after the beginning of high-glucose application) and lasted for several minutes before return to baseline membrane potential.

Two types of glucose responses were recorded: 19% of neurons (26 of 135) responded by a depolarization ( $3.6 \pm 0.3$  mV) and increased firing rate from  $2.1 \pm 0.3$  to  $4.5 \pm 0.5$  Hz (Fig. 4*A, left*). These glucosensing neurons had a mean membrane capacitance of  $40 \pm 4.5$  pF and input resistance ranging from  $200$  to  $1,300$  M $\Omega$ . Conversely, 7% of ARC neurons (9 of 135) were inhibited, i.e., they were hyperpolarized by  $4.6 \pm 0.9$  mV, and their firing rate decreased from  $2.1 \pm 0.6$  to  $0.6 \pm 0.3$  Hz in response to the  $5$ - to  $20$ -mmol/l glucose increase (Fig. 4*B, left*). These neurons had a mean membrane capacitance of  $24.2 \pm 3.4$  pF and input resistance ranging from  $430$  to  $1,700$  M $\Omega$ .

Because of the high-glucose concentrations used ( $5$  and  $20$  mmol/l), these two glucosensing neuron subtypes were, respectively, named high-glucose-excited (HGE) and high-glucose-inhibited (HGI) neurons. The percentage and response features of each subpopulation identified using cell-attached recording (which does not modify the cytosol) were not different from those identified using whole-cell recording (Fig. 4*A* and *B, right*).

Unfortunately, glucosensing neurons could not be identified a priori on the basis of their firing pattern at resting potential or membrane responses to hyperpolarizing current injection (Fig. 4*C*). In view of the low percentage of HGI neurons in the ARC, we decided to focus on the HGE neurons for the rest of the study.

**Glucose detection by HGE neurons.** To determine whether the glucose-induced excitation was direct or due to presynaptic inputs, the effect of a  $5$ - to  $20$ -mmol/l glucose increase was investigated when action potentials and thus synaptic transmission were blocked by TTX. The excitatory effect of the  $5$ - to  $20$ -mmol/l glucose increase persisted in the presence of TTX in all HGE neurons tested (6 of 6; Fig. 5*A*), without any significant modification in glucose-induced depolarization ( $20$  mmol/l glucose,  $3.4 \pm 0.5$  mV vs.  $20$  mmol/l glucose + TTX,  $3.6 \pm 0.2$  mV;  $n = 6$ ;  $P > 0.05$ ; Fig. 5*B*). These results suggest that HGE neurons directly detect an increase of glucose concentration from  $5$  to  $20$  mmol/l.

**Mechanism of glucose-induced HGE neuron depolarization.** The input resistance of HGE neurons was measured before and during glucose responses by recording the membrane potential change in response to a constant hyperpolarizing current injection (Fig. 4*A, left*). Depolarization of HGE neurons was correlated with a significant decrease of input resistance ( $24.3 \pm 4\%$ ,  $n = 13$ ; Fig. 6*A*), indicating membrane conductance increase.

Voltage-current ( $V$ - $I$ ) relations were extrapolated from increasing hyperpolarizing current ( $-5$  to  $-50$  pA) injected before and during glucose responses to identify ionic conductance involved. The glucose-induced current reversed at  $-23 \pm 6$  mV ( $n = 6$ ; Fig. 6*B*). Voltage-clamp recordings applying depolarizing voltage ramps (from  $-100$  to  $-15$  mV) confirmed this result, as shown in Fig. 6*B, inset*.

The reversal potential of glucose response was different from  $E_K$  in our solutions ( $-96$  mV) and did not correspond to any other equilibrium potential. Thus, these results

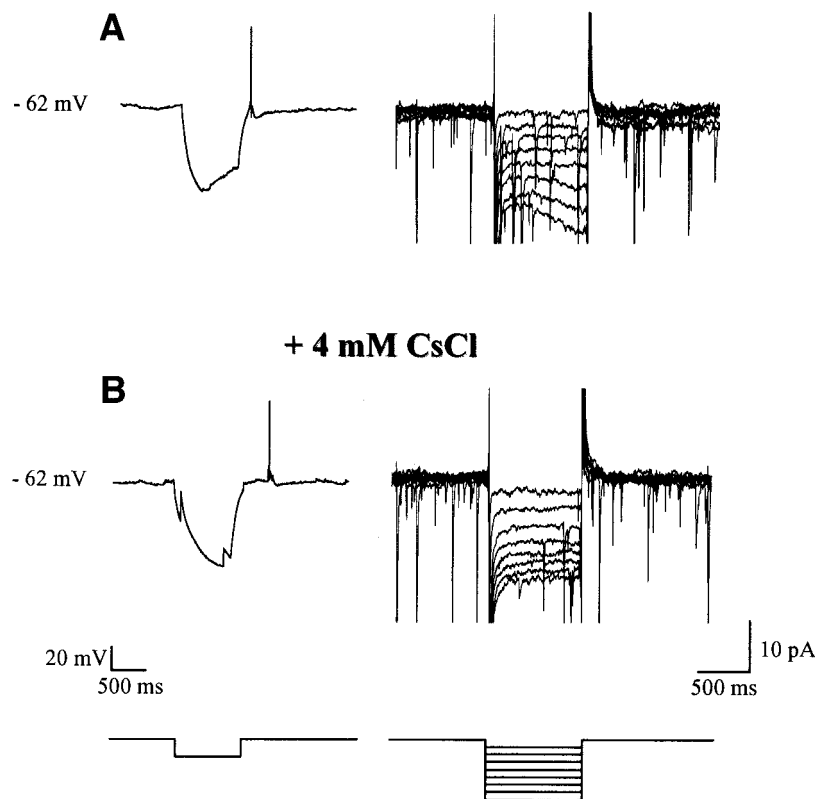


**FIG. 3.** A Cs<sup>+</sup>-sensitive  $I_h$  current is present in ARC neurons. Left and right traces are recordings from the same neuron made in the current- and voltage-clamp mode, respectively. *Left:* Membrane response to a -20 pA hyperpolarizing current. *Right:* Currents elicited by voltage steps from -70 to -150 mV from a resting potential of -65 mV. *A and B:* Recordings in the absence and in the presence of 4 mmol/l CsCl, respectively.

suggest that a 5- to 20-mmol/l glucose increase induced depolarization of HGE neurons through the opening of a nonselective cationic conductance.

**State of K<sub>ATP</sub> channels at 5 mmol/l glucose concentration.** The usual hypothesis for glucose-induced neuron excitation involves K<sub>ATP</sub> channel closure. Because our results were not in agreement with closure of K<sup>+</sup> channels, it was important to ascertain their presence and state (opened or closed) in ARC neurons in our experimental conditions. Therefore, we tested the effect of K<sub>ATP</sub> channel openers (pinacidil and diazoxide) and blockers (tolbutamide) on glucose-insensitive and HGE neurons with an extracellular glucose concentration of 5 mmol/l.

Application of pinacidil and diazoxide (both at 250 μmol/l) inhibited 8 of 10 glucose-insensitive neurons (Fig. 7A) and 5 of 5 HGE neurons (Fig. 7B and C, ■). K<sub>ATP</sub> channel openers hyperpolarized ARC neurons by ~9 mV (Fig. 7C) with decrease of firing rate at ~97% (Fig. 7B). Tolbutamide (250 μmol/l) reversed this inhibition and depolarized ARC neurons by ~3 mV with an increase of action potential frequency of 17% above basal activity. Nevertheless, the magnitude of tolbutamide response was much smaller than in response to pinacidil and diazoxide (Fig. 7B and C). Cell-attached recordings confirmed whole-cell results (data not shown). Taken together, these results suggest that 1) most ARC neurons have functional K<sub>ATP</sub> channels and 2) these channels are closer to the closed than the open state in 5 mmol/l glucose.

**Presence of HGE neurons in the ARC of Kir6.2 null mice.** To confirm that closure of the K<sub>ATP</sub> channel does not mediate the glucose excitatory effect on HGE neurons, we tested for their presence in the ARC of Kir6.2 null mice. Three of 15 ARC neurons were excited by a 5- to 20-mmol/l

glucose increase with an input resistance decrease (Fig. 8A). The reversal potential for the glucose response was the same as in the wild-type mice ( $n = 2$ , Fig. 8B). Thus, the ability to sense an increase in extracellular glucose concentration from 5 to 20 mmol/l persists in ARC HGE neurons of K<sub>ATP</sub> channel-deficient mice.

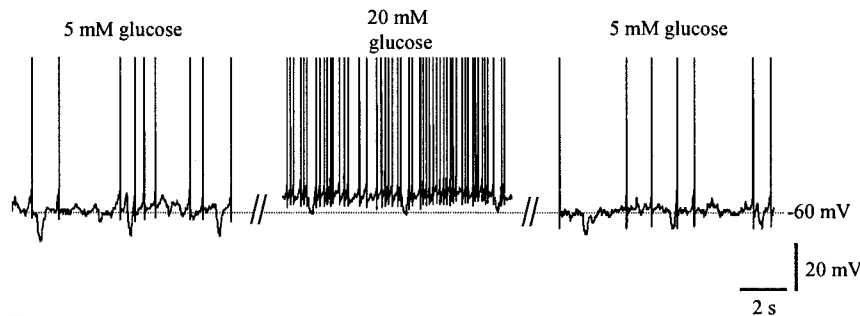
## DISCUSSION

After characterization of biophysical properties of ARC neurons, we investigated their sensitivity to an increase from 5 to 20 mmol/l in extracellular glucose concentration. We then focused on the glucose-excited neurons and studied the mechanism by which these neurons are stimulated by glucose.

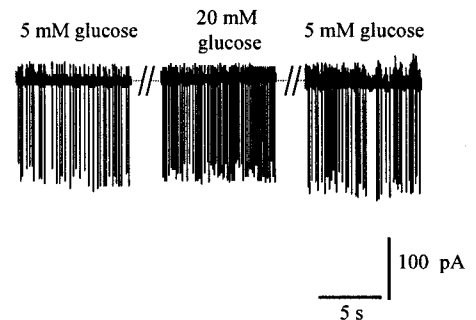
Whole-cell recordings revealed the presence of numerous spontaneously active ARC neurons and important presynaptic excitatory and/or inhibitory inputs as previously described (33,34). Investigation of membrane properties revealed five distinct phenotypes in response to hyperpolarizing current injection: type A neurons, which immediately resume firing at the end of current injection; type B neurons, which exhibit rebound depolarization; type C neurons, which display a rebound hyperpolarization; type D neurons, which exhibit a "sag" in membrane potential; and type E neurons, which display a "sag" in membrane potential and a rebound depolarization. Types A, B, and C have already been described in the ARC, but the presence of an  $I_h$  current underlying the "sag" in membrane potential (in neuron types D and E) was more controversial (22,32,35). Our results in the anterior ARC are consistent with those of Poulain's and Ibrahim's groups describing the presence of "sag" and/or  $I_h$  current

## A High glucose-excited (HGE) neurons

### Whole-cell

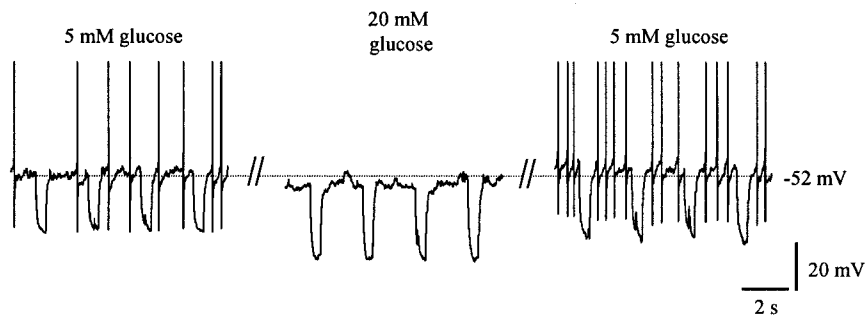


### Cell-attached

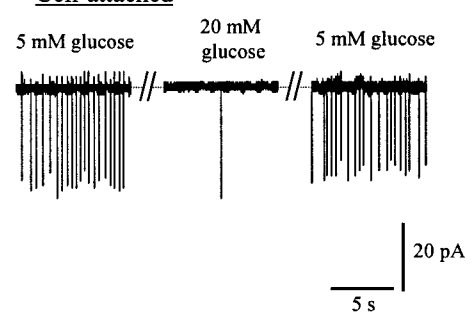


## B High glucose-inhibited (HGI) neurons

### Whole-cell



### Cell-attached



## C Properties of HGE and HGI neurons

	“Type A” neurons No rebound potential	“Type B” neurons Rebound depolarization	“Type C” neurons Rebound hyperpolarization	“Type D” neurons Sag	“Type E” neurons Rebound depolarization + Sag
<b>HGE neurons (n = 21)</b>	13 %	25 %	4 %	4 %	54 %
<b>HGI neurons (n = 9)</b>	22 %	44 %	22 %	11 %	0 %

FIG. 4. Glucose excites as well as inhibits ARC neurons. A 5- to 20-mmol/l glucose increase modified the firing frequency of glucosensing neurons. A and B: Representative examples of HGE and HGI neurons, respectively. Whole-cell (left) and cell-attached (right) configurations were used. Downward deflections in whole-cell current-clamp recordings represent the membrane voltage responses to constant hyperpolarizing currents. C: HGE and HGI neurons are found in most ARC subpopulations.

in ARC. This disagreement with the data from Burdakov and Ashcroft may be because they evaluated the posterior ARC (32,36). The finding of  $I_h$  channel expression in ARC reinforces our results (37). The  $I_h$  current in anterior ARC neurons may control neuronal activity 1) by determining resting membrane potential, 2) by regulating the response to hyperpolarization such as during arrival of inhibitory synaptic potentials that are numerous in ARC (33,34, and unpublished personal observations), and 3) by contributing to “pacemaker” activity also present in ARC (35,38, and our study).

The second part of the present study clearly demonstrates the presence of ARC glucosensing neurons that

respond to increased extracellular glucose concentration from 5 to 20 mmol/l. These data are very important because previous studies have evaluated ARC glucosensing neurons mainly in response to large nonphysiological steps in extracellular glucose (i.e., from 0 to 10 or 20 mmol/l) or to a glucose level <5 mmol/l (7,14,15). However, there is a paucity of data regarding the responses of ARC glucosensing neurons as glucose levels are raised above 5 mmol/l. This is because the majority of studies measuring brain glucose levels suggest that, in general, they are ~30% that of plasma glucose, ranging from 0.1 to 4.5 mmol/l for hypo- to hyperglycemic states, with a set point at ~2.5 mmol/l (27,39,40). However, actual glucose

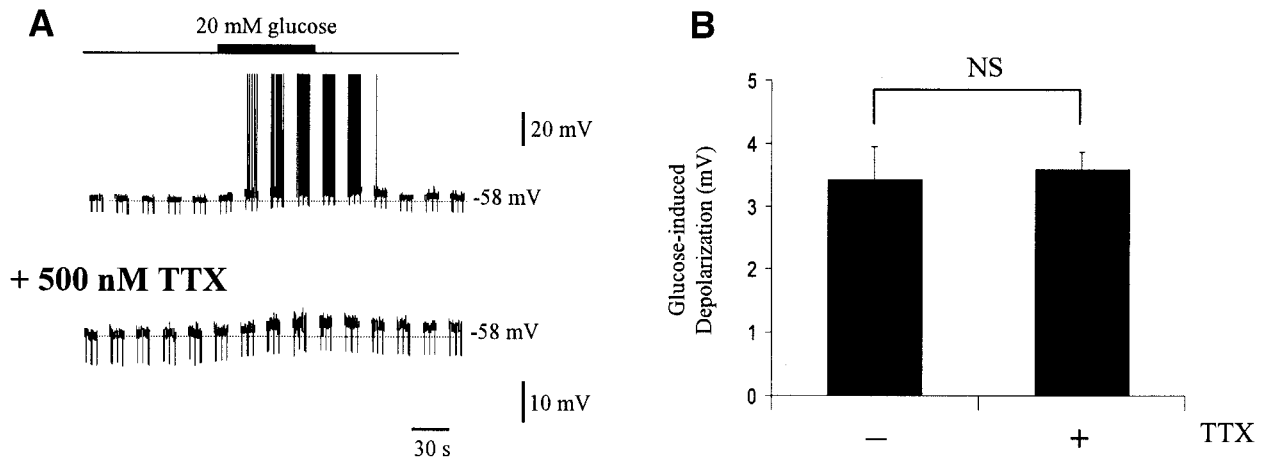


FIG. 5. Glucose detection by HGE neurons is direct. *A*: Membrane potential was followed by 10-s recording sweeps. Glucose at 20 mmol/l was applied twice on the same HGE neuron in the absence (*top*) or in the presence (*bottom*) of 500 nmol/l TTX. *B*: TTX treatment did not modify glucose-induced depolarization. NS:  $P > 0.05$ .

levels in the ARC are more controversial because of its proximity to the median eminence, where the blood-brain barrier is "leaky" (5). Thus, it is reasonable to hypothesize that extracellular glucose concentration in the ARC may approximate plasma level and exceed 4.5 mmol/l. Moreover, like in the pancreatic  $\beta$ -cells, glucokinase plays a role in central nervous system glucosensing (41) and is functional mainly in the range  $>5$  mmol/l (42). Therefore, for these reasons, we used a basal glucose concentration of 5 mmol/l and an increase to 20 mmol/l. With this glucose step, we recorded glucose-insensitive neurons and neurons that can be either excited or inhibited. By analogy to the definitions of Song et al. (16), for our higher glucose concentrations, these last two neuron subpopulations were called HGE and HGI neurons.

To our knowledge, this is the first study clearly investigating the proportion of neurons that are sensitive to high-glucose changes in mouse ARC. Compared with Yang et al. (28,29), who used the same glucose step in rat VMH, the proportion of glucosensing neurons in the ARC is

similar for HGE but lower for HGI neurons. The proportion found in the present study is equivalent to that reported by Wang et al. (7) for glucose-excited and -inhibited neurons in the rat ARC using extracellular glucose changes from 2.5 to 0.1 or 5 mmol/l. Because we did not evaluate glucose levels  $<5$  mmol/l, we cannot conclude whether these glucose-excited and -inhibited neurons may correspond to HGE and HGI neurons. Nevertheless, we can speculate that glucose-excited and HGE neurons form two subpopulations. Indeed, HGE neurons show a large change in firing rate in response to a 5- to 20-mmol/l glucose step, whereas action potential frequency of glucose-excited neurons plateaus above 2.5 mmol/l (7). Glucose-inhibited and HGI ARC neurons also seem to be different cells. Indeed, HGI neurons present spontaneous action potentials at 5 mmol/l glucose, whereas glucose-inhibited neurons are mostly quiescent above 2.5 mmol/l glucose (V.H. Routh, personal communication).

We next investigated the mechanism involved in high-glucose detection by HGE neurons. Inhibition of synaptic

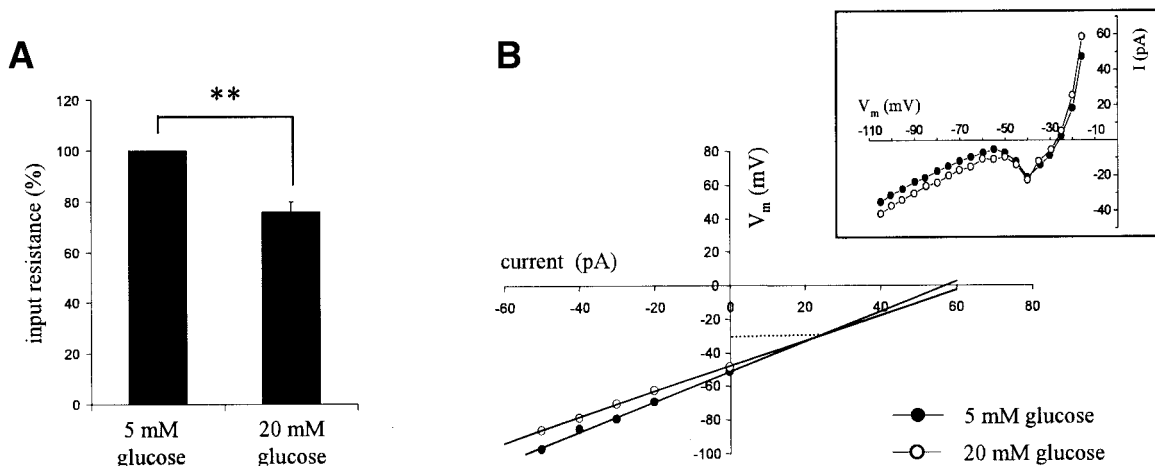
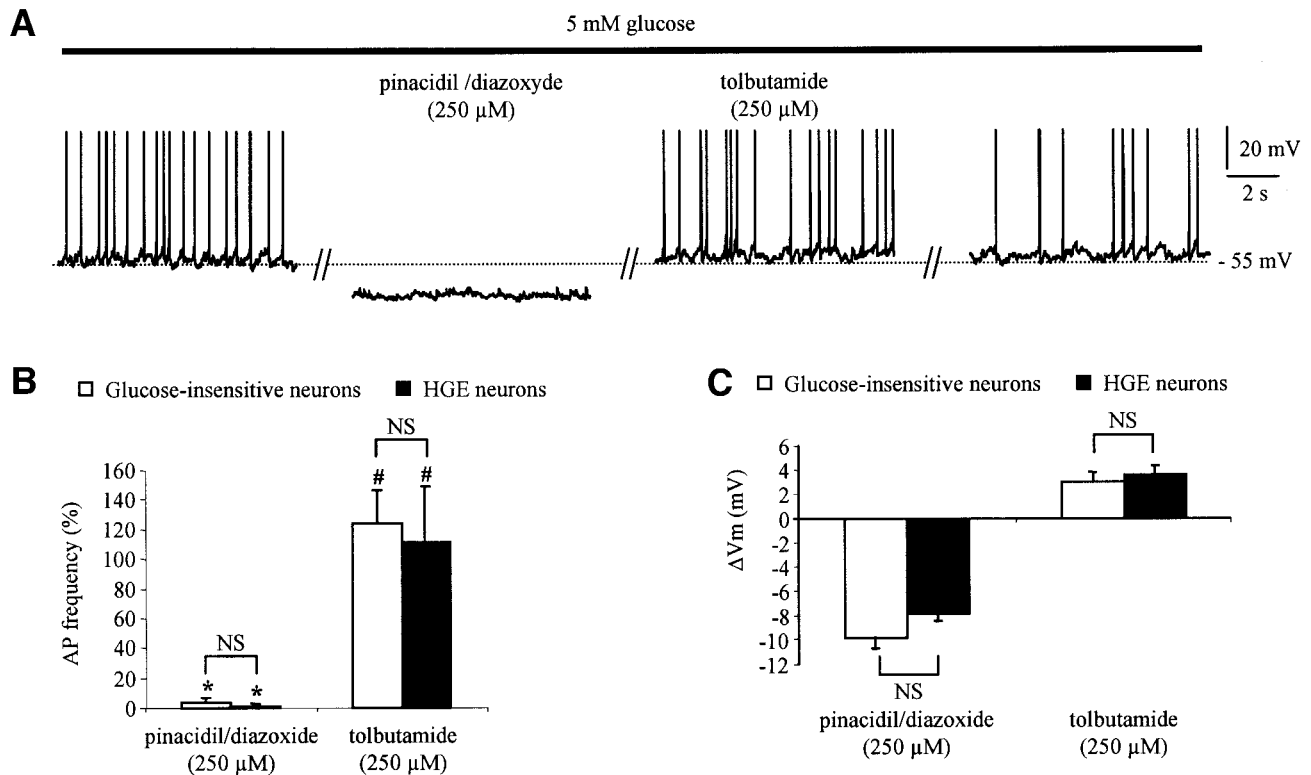


FIG. 6. The glucose-induced excitation involved a nonspecific cationic conductance. *A*: High-glucose application decreases input resistance, which was obtained by measuring membrane potential changes in response to hyperpolarizing current pulse. Input resistance before glucose application was taken as 100%. \*\* $P < 0.0005$ . *B*: Representative voltage-current curve derived from membrane potential responses to increasing hyperpolarizing current steps before (●) and during (○) 20 mmol/l glucose application. The reversal potential was close to  $-20$  mV, as indicated by the dotted line. *Inset*: Representative current-voltage relationship obtained by applying voltage-ramps before and during glucose-induced response.



**FIG. 7.**  $K_{ATP}$  channels are mostly closed at 5 mmol/l glucose concentration. **A:** Pinacidil and diazoxide (250  $\mu$ mol/l both) hyperpolarized a glucose-insensitive neuron. This inhibition was reversed by tolbutamide (250  $\mu$ mol/l). **B:** Quantification of pinacidil-diazoxide and tolbutamide effects on firing rate. Action potential frequencies in resting conditions were taken as 100%. NS:  $P > 0.05$ ; #  $P > 0.05$  versus resting conditions; \*  $P < 0.05$  versus resting conditions. **C:** Pinacidil-diazoxide and tolbutamide effects on membrane potential. Data are expressed as differences ( $\Delta V_m$ ) from resting membrane potential. NS:  $P > 0.05$ .

transmission by TTX does not modify HGE neuron response, thus suggesting a direct glucose detection. Similar results were also found by Wang et al. (7) for rat ARC glucose-excited neurons. However, in the VMN, detection of a glucose increase above 2.5 mmol/l is due to presynaptic inputs (16). Thus, HGE and HGI neurons may provide the presynaptic regulation of VMN neurons in response to high glucose described by Song et al. (16). These data are consistent with those concerning the

neuropeptide Y and pro-opiomelanocortin neuronal networks (1,2), which suggest that the ARC may be the first nucleus to detect peripheral metabolic signals and then relay this information to other hypothalamic nuclei such as VMN or PVN (paraventricular nucleus).

Over the past 15 years, it has been demonstrated that  $K_{ATP}$  channel closure is a key step in cerebral glucosensing (13,28,43). Recent studies, using extracellular glucose changes at  $\sim 2.5$  mmol/l, show that glucose-induced acti-

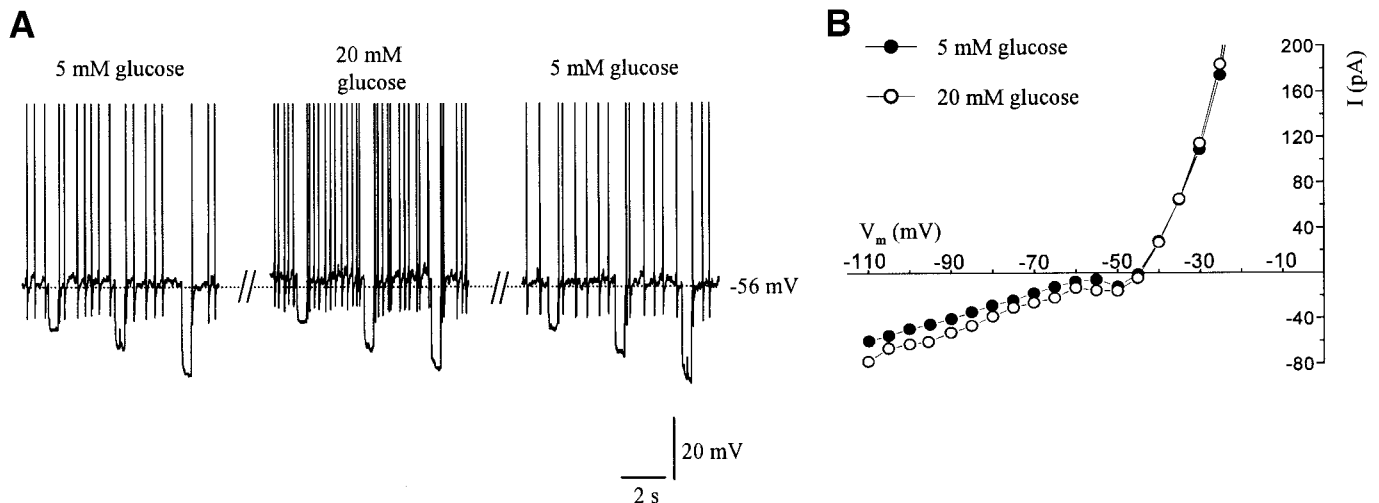


**FIG. 8.** HGE neurons are found in the ARC of Kir6.2 null mice. **A:** A 5- to 20-mmol/l glucose increase depolarized membrane potential and increased firing rate. **B:** Current-voltage relationship before (●) and during (○) 20 mmol/l glucose application.

vation of VMN or ARC glucose-excited neurons is correlated to a decrease of K<sup>+</sup> conductance (7,16). Moreover, Miki et al. (44) failed to detect glucosensing neurons in the VMN of K<sub>ATP</sub> channel-deficient mice. These results point out that the glucose sensitivity, at least at ~2.5 mmol/l, depends on K<sub>ATP</sub> channel activity. However, for glucose concentrations >5 mmol/l, we show a different mechanism for glucose activation of HGE neurons: first, the glucose-induced depolarization was correlated to a significant decrease of input resistance, indicating an increase of membrane conductance. Moreover, our results and others (19,22) have demonstrated that K<sub>ATP</sub> channels were present and functional in ARC neurons. However, in glucose-insensitive neurons as well as in HGE neurons, these K<sub>ATP</sub> channels were mostly closed at 5 mmol/l extracellular glucose concentration. This is consistent with the work of Wang et al. (7), which shows that the decrease in K<sub>ATP</sub> channel current in response to increase from 0.1 to 10 mmol/l plateaus above 2.5 mmol/l. Finally, we identified ARC HGE neurons in Kir6.2 knockout mice. The number and the responses of these HGE neurons were similar to those obtained in wild-type mice. These results agree with other studies suggesting a likely additional mechanism independent of K<sub>ATP</sub> channels, as it has been demonstrated in pancreatic  $\beta$ -cells (23–25). Indeed, the presence of K<sub>ATP</sub> channels is not entirely correlated to glucose-induced neuronal response (21). Furthermore, an increase in glucose concentration from 3 to 15 mmol/l did not significantly modify intracellular ATP levels in VMH neurons (45). Finally, the K<sub>ATP</sub> channel opener diazoxide blocked only the 5 to 20 mmol/l glucose effect in a minority of glucose-excited neurons in rat VMH, clearly calling into question the importance of K<sub>ATP</sub> channels. In this later study, the authors suggested that, instead of ATP, the key metabolic signal would be NADH (26,28). Taken together, these data give clear evidence that, at glucose concentrations >5 mmol/l, a K<sub>ATP</sub> channel-independent mechanism mediates glucose-induced excitation of ARC HGE neurons.

Current- and voltage-clamp recordings suggested that a nonselective cationic conductance mediates depolarization of HGE neurons. Indeed, we showed that the glucose-activated conductance reversed at a potential close to -20 mV, which is different from the K<sup>+</sup> equilibrium potential. A similar conductance has been described for orexin and leptin in hypothalamic neurons (6,46). It is tempting to speculate that this cationic conductance may be a common target for different metabolic signals.

In conclusion, we show that ARC neurons are capable of sensing increased extracellular glucose levels >5 mmol/l. These neurons may play a role in regulation of hyperglycemia. Activation of HGE and HGI neurons could lead to modulation of autonomic nervous system activity and, as a consequence, peripheral glucose homeostasis regulation (47). The second important point of our results is the demonstration of a new, additional K<sub>ATP</sub> channel-independent mechanism in glucose detection. This feature argues for similarity between ARC and pancreatic glucosensing. The nature of the cationic conductance and the mechanisms by which high-glucose concentration activates it remain to be determined. However, this pathway may represent a novel brain “molecular glucosensor.”

## ACKNOWLEDGMENTS

X.F. was supported by a fellowship from the Ministère de la Recherche et de la Technologie. This work was funded in part by grants from the CNRS, awarded to A.L. (crédit de soutien aux jeunes équipes no. 01N60/0787).

We are indebted to J.-M. Lerne for involvement in mice care and very grateful to G. Portolan and M. Belliure for technical help in immunohistochemistry. We thank Dr. V. Routh for helpful discussions and critical reading of the final manuscript. We are grateful to Dr. S. Seino for providing Kir6.2 null mice.

## REFERENCES

1. Elmquist JK, Elias CF, Saper CB: From lesions to leptin: hypothalamic control of food intake and body weight. *Neuron* 22:221–232, 1999
2. Schwartz MW, Woods SC, Porte D Jr, Seeley RJ, Baskin DG: Central nervous system control of food intake. *Nature* 404:661–671, 2000
3. Barsh GS, Farooqi IS, O'Rahilly S: Genetics of body-weight regulation. *Nature* 404:644–651, 2000
4. Kalra SP, Dube MG, Pu S, Xu B, Horvath TL, Kalra PS: Interacting appetite-regulating pathways in the hypothalamic regulation of body weight. *Endocr Rev* 20:68–100, 1999
5. Ganong WF: Circumventricular organs: definition and role in the regulation of endocrine and autonomic function. *Clin Exp Pharmacol Physiol* 27:422–427, 2000
6. Cowley MA, Smart JL, Rubinstein M, Cerdan MG, Diano S, Horvath TL, Cone RD, Low MJ: Leptin activates anorexigenic POMC neurons through a neural network in the arcuate nucleus. *Nature* 411:480–484, 2001
7. Wang R, Liu X, Hentges ST, Dunn-Meynell AA, Levin BE, Wang W, Routh VH: The regulation of glucose-excited neurons in the hypothalamic arcuate nucleus by glucose and feeding-relevant peptides. *Diabetes* 53:1959–1965, 2004
8. Pénicaud L, Leloup C, Lorsignol A, Alquier T, Guillod E: Brain glucose sensing mechanism and glucose homeostasis. *Curr Opin Clin Nutr Metab Care* 5:539–543, 2002
9. Atef N, Ktorza A, Pénicaud L: CNS involvement in the glucose induced increase of islet blood flow in obese Zucker rats. *Int J Obes Relat Metab Disord* 19:103–107, 1995
10. Guillod-Maximin E, Lorsignol A, Alquier T, Pénicaud L: Acute intracarotid glucose injection towards the brain induces specific *c-fos* activation in hypothalamic nuclei: involvement of astrocytes in cerebral glucose-sensing in rats. *J Neuroendocrinol* 16:464–471, 2004
11. Anand BK, Chhina GS, Sharma KN, Dua S, Singh B: Activity of single neurons in the hypothalamic feeding centers: effect of glucose. *Am J Physiol* 207:1146–1154, 1964
12. Oomura Y, Yoshimatsu H: Neural network of glucose monitoring system. *J Auton Nerv Syst* 10:359–372, 1984
13. Ashford ML, Boden PR, Treherne JM: Glucose-induced excitation of hypothalamic neurones is mediated by ATP-sensitive K<sup>+</sup> channels. *Pflugers Arch* 415:479–483, 1990
14. Spanswick D, Smith MA, Groppi VE, Logan SD, Ashford ML: Leptin inhibits hypothalamic neurons by activation of ATP-sensitive potassium channels. *Nature* 390:521–525, 1997
15. Spanswick D, Smith MA, Mirshamsi S, Routh VH, Ashford ML: Insulin activates ATP-sensitive K<sup>+</sup> channels in hypothalamic neurons of lean, but not obese rats. *Nat Neurosci* 3:757–758, 2000
16. Song Z, Levin BE, McArdle JJ, Bakhos N, Routh VH: Convergence of pre- and postsynaptic influences on glucosensing neurons in the ventromedial hypothalamic nucleus. *Diabetes* 50:2673–2681, 2001
17. Levin BE, Dunn-Meynell AA, Routh VH: Brain glucosensing and the K(ATP) channel. *Nat Neurosci* 4:459–460, 2001
18. Schuit FC, Huypens P, Heimberg H, Pipeleers DG: Glucose sensing in pancreatic  $\beta$ -cells: a model for the study of other glucose-regulated cells in gut, pancreas, and hypothalamus. *Diabetes* 50:1–11, 2001
19. Dunn-Meynell AA, Rawson NE, Levin BE: Distribution and phenotype of neurons containing the ATP-sensitive K<sup>+</sup> channel in rat brain. *Brain Res* 814:41–54, 1998
20. Lee K, Dixon AK, Richardson PJ, Pinnock RD: Glucose-receptive neurones in the rat ventromedial hypothalamus express KATP channels composed of Kir6.1 and SUR1 subunits. *J Physiol* 515:439–452, 1999
21. Kang L, Routh VH, Kuzhikandathil EV, Gaspers LD, Levin BE: Physiological and molecular characteristics of rat hypothalamic ventromedial nucleus glucosensing neurons. *Diabetes* 53:549–559, 2004

22. Ibrahim N, Bosch MA, Smart JL, Qiu J, Rubinstein M, Ronnekleiv OK, Low MJ, Kelly MJ: Hypothalamic proopiomelanocortin neurons are glucose responsive and express K(ATP) channels. *Endocrinology* 144:1331–1340, 2003
23. Gembal M, Gilon P, Henquin JC: Evidence that glucose can control insulin release independently from its action on ATP-sensitive K<sup>+</sup> channels in mouse B cells. *J Clin Invest* 89:1288–1295, 1992
24. Aizawa T, Komatsu M, Asanuma N, Sato Y, Sharp GW: Glucose action 'beyond ionic events' in the pancreatic beta cell. *Trends Pharmacol Sci* 19:496–499, 1998
25. Eto K, Tsubamoto Y, Terauchi Y, Sugiyama T, Kishimoto T, Takahashi N, Yamauchi N, Kubota N, Murayama S, Aizawa T, Akanuma Y, Aizawa S, Kasai H, Yazaki Y, Kadowaki T: Role of NADH shuttle system in glucose-induced activation of mitochondrial metabolism and insulin secretion. *Science* 283:981–985, 1999
26. Mobbs CV, Kow LM, Yang XJ: Brain glucose-sensing mechanisms: ubiquitous silencing by aglycemia vs. hypothalamic neuroendocrine responses. *Am J Physiol Endocrinol Metab* 281:E649–E654, 2001
27. Silver IA, Erecinska M: Extracellular glucose concentration in mammalian brain: continuous monitoring of changes during increased neuronal activity and upon limitation in oxygen supply in normo-, hypo-, and hyperglycemic animals. *J Neurosci* 14:5068–5076, 1994
28. Yang XJ, Kow LM, Funabashi T, Mobbs CV: Hypothalamic glucose sensor: similarities to and differences from pancreatic beta-cell mechanisms. *Diabetes* 48:1763–1772, 1999
29. Yang XJ, Kow LM, Pfaff DW, Mobbs CV: Metabolic pathways that mediate inhibition of hypothalamic neurons by glucose. *Diabetes* 53:67–73, 2004
30. Miki T, Nagashima K, Tashiro F, Kotake K, Yoshitomi H, Tamamoto A, Gono T, Iwanaga T, Miyazaki J, Seino S: Defective insulin secretion and enhanced insulin action in KATP channel-deficient mice. *Proc Natl Acad Sci U S A* 95:10402–10406, 1998
31. Paxinos G, Franklin KBJ: *The Mouse Brain in Stereotaxic Coordinates*. New York, Academic Press, 1997
32. Burdakov D, Ashcroft FM: Cholecystokinin tunes firing of an electrically distinct subset of arcuate nucleus neurons by activating A-type potassium channels. *J Neurosci* 22:6380–6387, 2002
33. Belousov AB, van den Pol AN: Local synaptic release of glutamate from neurons in the rat hypothalamic arcuate nucleus. *J Physiol* 499 (Suppl.): 747–761, 1997
34. Pinto S, Roseberry AG, Liu H, Diano S, Shanabrough M, Cai X, Friedman JM, Horvath TL: Rapid rewiring of arcuate nucleus feeding circuits by leptin. *Science* 304:110–115, 2004
35. Poulain P, Decroq N, Mitchell V: Direct inhibitory action of galanin on hypothalamic arcuate nucleus neurons expressing galanin receptor Gal-r1 mRNA. *Neuroendocrinology* 78:105–117, 2003
36. Burdakov D, Liss B, Ashcroft FM: Orexin excites GABAergic neurons of the arcuate nucleus by activating the sodium-calcium exchanger. *J Neurosci* 23:4951–4957, 2003
37. Monteggia LM, Eisch AJ, Tang MD, Kaczmarek LK, Nestler EJ: Cloning and localization of the hyperpolarization-activated cyclic nucleotide-gated channel family in rat brain. *Brain Res Mol Brain Res* 81:129–139, 2000
38. Van Den Top M, Lee K, Whyment AD, Blanks AM, Spanwick D: Orexin-sensitive NPY/AgRP pacemaker neurons in the hypothalamic arcuate nucleus. *Nat Neurosci* 7:493–494, 2004
39. McNay EC, Gold PE: Extracellular glucose concentrations in the rat hippocampus measured by zero-net-flux: effects of microdialysis flow rate, strain, and age. *J Neurochem* 72:785–790, 1999
40. de Vries MG, Arseneau LM, Lawson ME, Beverly JL: Extracellular glucose in rat ventromedial hypothalamus during acute and recurrent hypoglycemia. *Diabetes* 52:2767–2773, 2003
41. Dunn-Meynell AA, Routh VH, Kang L, Gaspers L, Levin BE: Glucokinase is the likely mediator of glucosensing in both glucose-excited and glucose-inhibited central neurons. *Diabetes* 51:2056–2065, 2002
42. Matschinsky FM, Glaser B, Magnuson MA: Pancreatic beta-cell glucokinase: closing the gap between theoretical concepts and experimental realities. *Diabetes* 47:307–315, 1998
43. Levin BE: Glucosensing neurons do more than just sense glucose. *Int J Obes Relat Metab Disord* 25 (Suppl. 5):S68–S72, 2001
44. Miki T, Liss B, Minami K, Shiuchi T, Saraya A, Kashima Y, Horiuchi M, Ashcroft F, Minokoshi Y, Roeper J, Seino S: ATP-sensitive K<sup>+</sup> channels in the hypothalamus are essential for the maintenance of glucose homeostasis. *Nat Neurosci* 4:507–512, 2001
45. Ainscow EK, Mirshamsi S, Tang T, Ashford ML, Rutter GA: Dynamic imaging of free cytosolic ATP concentration during fuel sensing by rat hypothalamic neurones: evidence for ATP-independent control of ATP-sensitive K(+) channels. *J Physiol* 544:429–445, 2002
46. Follwell MJ, Ferguson AV: Cellular mechanisms of orexin actions on paraventricular nucleus neurones in rat hypothalamus. *J Physiol* 545:855–867, 2002
47. Pénicaud L, Cousin B, Leloup C, Lorsignol A, Casteilla L: The autonomic nervous system, adipose tissue plasticity, and energy balance. *Nutrition* 16:903–908, 2000